Supplementary Materials

EXPERIMENTS

Materials

Zirconium chloride（$ZrCl_4$, ≥98%）, triethylamine (TEA， ≥99.5%), and anhydrous piperazine (PIP, ≥99%) were procured from Shanghai Aladdin Biochemical Technology Co., Ltd., China. 1,4-Dicarboxybenzene (ligands, ≥99%) and 2-aminoterephthalic acid (ligands, ≥98%) was obtained from Shanghai Dibo Biotechnology Co., Ltd., China. 1,3,5-Benzenetricarbonyl trichloride (TMC, 98%), congo red (CR, M_w = 696.68 g·mol^{-1}), methyl blue (MeB, M_w = 799.80 g·mol^{-1}), methylene blue (MB, M_w = 319.85 g·mol^{-1}), and methyl orange (MO, M_w = 327.33 g·mol^{-1}) was purchased from Shanghai Macklin Biochemical Technology Co., Ltd., China. Anhydrous methanol, N,N-dimethylformamide (DMF), and n-Hexane were procured from Sinopharm Chemical Reagent Co., Ltd., China. Deionized water was taken from the laboratory water purification system. The polysulfone (PSf) membrane was purchased from Beijing Saipurite Equipment Co., Ltd., China. All chemicals are used as supplied without further purification. Polysulfone (PSf) ultrafiltration membranes (mean pore diameter, 20–30 nm) were obtained from Shandong Jiuzhang Membrane Technology Co., Ltd. (China) and immersed in deionized water for 12 h before use.

Preparation of UiO-66 and UiO-66-NH_2

UiO-66 was synthesized as follows: $ZrCl_4$ (0.0424 g, 0.182 mmol) and 1,4-benzenedicarboxylic acid (0.0302 g, 0.363 mmol) were dissolved in 21 mL (272 mmol) of DMF and ultrasonicated for 30 min. The resulting mixture was transferred into a Teflon-lined stainless steel autoclave of 30 mL capacity and maintained at 393 K for 24 h. After completion, the autoclave was cooled to room temperature in air. The resulting solid was filtered, washed three times with DMF, then six times with methanol, and dried in a vacuum oven at 333 K for 10 h to obtain UiO-66 [S1].

Similarly, UiO-66-NH_2 was synthesized using the identical procedure, except that the ligand was replaced with an equimolar amount of 2-aminoterephthalic acid.

Preparation of TFN Membrane

Firstly, the aqueous phase solution was prepared by completely dissolving 1 wt% PIP and 1 wt% TEA in ultrapure water, while the organic phase solution was prepared by dissolving 0.1 wt% TMC in n-hexane. Both phases were stirred separately until complete dissolution. Both two-phase solutions were freshly prepared and used immediately. Subsequently, a wet PSf membrane was placed on a clean glass plate (with the membrane face up) and fixed with a plastic frame, and residual water droplets on the membrane surface were blown off using an air knife. The aqueous phases was then poured onto the membrane surface and allowed to remain for 3 min, after which the excess aqueous phase was poured off, and a rubber roller was employed to remove any residual solution from the surface. Subsequently, the organic phase solution was slowly poured onto the PSf membrane surface, reacted for 1 min, and the excess TMC solution was decanted. Interfacial polymerization formed the NF membrane, which was rinsed with n-hexane. Finally, the membrane was placed in an oven at 338 K for 6 min, after which it was removed and immersed in deionized water for storage, and was denoted as the TFN-0 membrane.

The preparation process for TFN membranes is identical to that for TFN-0 membranes. The difference is that PIP (1 wt%), TEA (1 wt%) and UiO-66-NH_2 (0.05, 0.10, 0.15, 0.20 wt%) are dissolved in deionized water to prepare an aqueous solution, and then ultrasonically dispersed for 30 minutes to ensure uniform distribution of UiO-66-NH_2. The membranes containing UiO-66-NH_2 were denoted as the TFN-0.05, TFN-0.1, TFN-0.15, and TFN-0.2 membranes, respectively.

Separation Performance of Membrane

The membrane water flux and dye rejection rate were evaluated using a cross-flow filtration setup, which featured three parallel circular filtration cells [S2]. The effective filtration area of the cell was 7.065 cm^2. All permeate and feed streams, except during sampling, were returned to the feed tank. The membrane was first compacted with deionized water at 0.5 MPa for 30 min to achieve a stable water flux, after which the pure water flux was measured

at the same pressure. Notably, prior to compaction, the membrane to be tested was stored immersed in deionized water. Each membrane was tested three times, and the average value was reported. Pure water flux (P, $L \cdot m^{-2} \cdot h^{-1}$) was calculated using Equation (1).

$$P = \frac{V}{A \times \Delta t} \quad (1)$$

where V is the volume of permeate (L), A is the effective membrane area (m^2), and Δt is the sampling time (h).

The dye rejection performance of the TFN membranes was determined using 0.1 g/L feed solutions of MeB, CR, MO, and MB at an operating pressure of 0.5 MPa. All dye solutions were treated with ultrasonication before use. Following the same procedure as the pure water flux test, all membranes were pre-compacted for 30 min prior to the dye rejection experiment. The concentrations of dyes in the feed and permeate solutions were analyzed by ultraviolet-visible (UV-Vis) spectroscopy. The separation performance of the composite membranes was evaluated using single-component dye solutions. The dye rejection (R, %) was calculated according to Equation (2).

$$R = (1 - \frac{C_p}{C_f}) \times 100\% \quad (2)$$

where C_p and C_f are the dye concentrations in the permeate and feed solutions, respectively.

Testing and Characterization

The surface chemical structures of UiO-66 and UiO-66-NH_2 were characterized by a Nicolet iS50 type Fourier transform infrared (FTIR) spectroscopy. The crystal structure of UiO-66-NH_2 was analyzed using a D8 ADVANCE type X-ray diffraction (XRD). The microscopic morphologies of UiO-66-NH_2 and the membranes were observed by a Gemini SEM500 type field emission scanning electron microscopy (FESEM). The specific surface area of UiO-66-NH_2 was determined on a Autosorb-iQ-C type BET surface area and pore size analyzer. The surface area was calculated by the Brunauer–Emmett–Teller (BET) method, and the pore size distribution was obtained via the HK method. The elemental composition and chemical states on the membrane surface were analyzed by a NEXSA type X-ray photoelectron spectroscopy (XPS). The chemical interactions between the MOF particles and the PA layer were verified by measuring the chemical shifts in the binding energies of characteristic elements (e.g., O and N) on the membrane surface. The surface elemental types, relative contents, and distribution corresponding to the microscopic morphology of the samples were analyzed using a EDAX type energy dispersive X-ray spectroscopy (EDS). The electrokinetic potential of the membrane surface was measured with a solid surface zeta potential analyzer. The static water contact angle of the membranes in air was measured using a DSA30S type water contact angle (WCA) goniometer. Each membrane sample was measured at least five times at different positions, and the average value was reported.

Table S1: Performance Comparison of Various Membranes for the Separation of dye (MeB, CR, MB, MO)

Membrane	Water Flux ($L \cdot m^{-2} \cdot h^{-1}$)	Dye	Rejection (%)	References
In-MOF@PVDF	398.73	MB	99	S3
		MO	39	
GO-PAA/PES	74	CR	91	S4
		MB	78	
Sm-MOF/GO	26	MB	91	S5
NATP-GCN/PSF	55.4	CR	88	S6
GO-GLU/TFN	14.11	MeB	99.18	S7
		MO	67.18	
UiO-66-NH_2/TFN	45.77	MeB	98.2	This work
		CR	98.5	
		MB	83	
		CO	75.6	

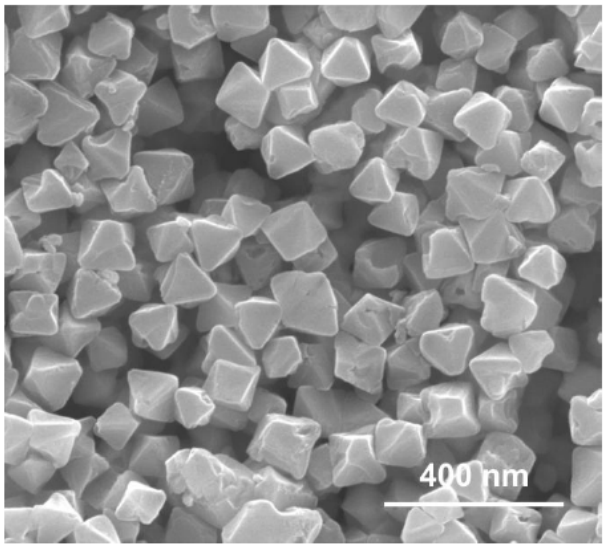

Figure S1: SEM images of UiO-66.

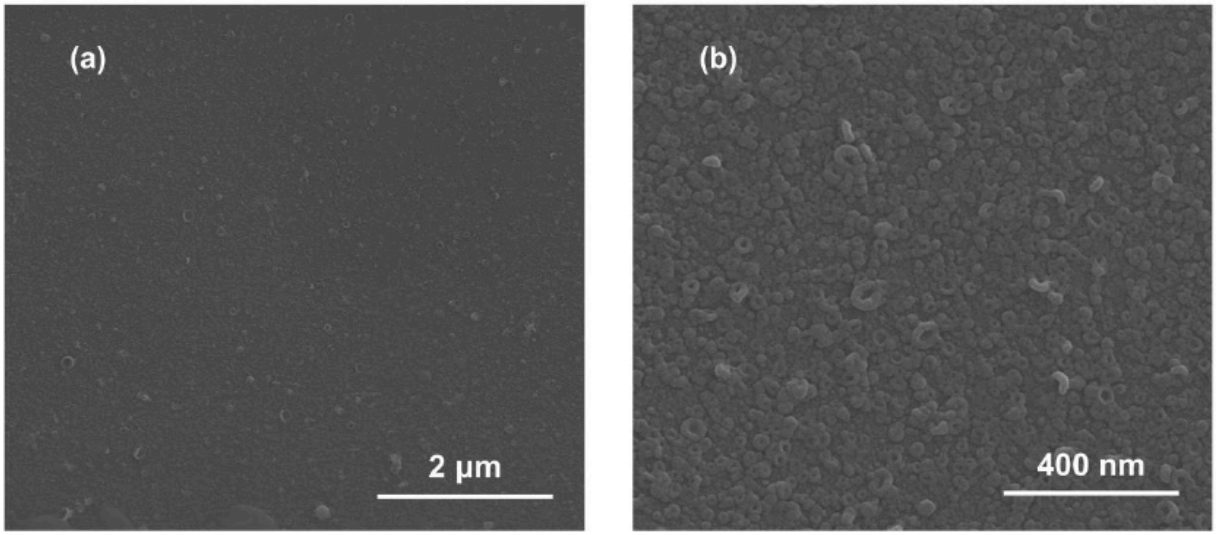

Figure S2: SEM images of TFN-0 memembrane.

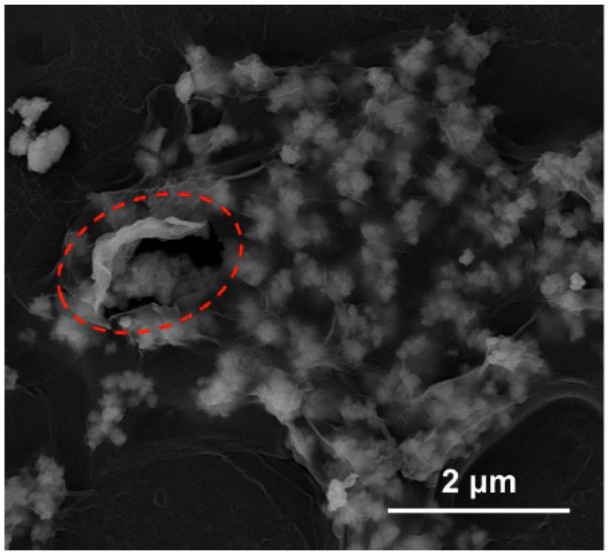

Figure S3: SEM images of TFN-U memembrane.

REFERENCES

[S1] Yu C, Cen X, Ao D, Qiao Z, Zhong C. Preparation of thin-film composite membranes with ultrahigh MOFs loading through polymer-template MOFs induction secondary interfacial polymerization. Appl Surf Sci 2023; 614: 156186. https://doi.org/10.1016/j.apsusc.2022.156186

[S2] Cao J, Ge J, Gao Y, Liao B. Impact of amino and methyl groups on the loading capacity of UiO-66 for 8-hydroxyquinoline: an in-depth experimental and computational analysis. RSC Adv 2025; 15: 20570-20588. https://doi.org/10.1039/D5RA02802G

[S3] Maru L, Kalla S, Jangir R. Efficient dye extraction from wastewater using indium-MOF immobilized polyvinylidene fluoride membranes with selective filtration for enhanced remediation. Langmuir 2024; 40: 8144-8161. https://doi.org/10.1021/acs.langmuir.4c00194

[S4] Khan IA, Khan AU, Butt MS, Janjua HA, Uddin E, Deen KM, Sadiq R, Ahmad NM. Dye removal from contaminated water through PES membranes enhanced with the incorporation of switchable polyacrylic acid grafted on graphene oxide. ACS Omega 2025; 10: 28178-28190. https://doi.org/10.1021/acsomega.5c02815

[S5] Yang G, Zhang D, Zhu G, Zhou T, Song M, Qu L, Xiong K, Li H. A Sm-MOF/GO nanocomposite membrane for efficient organic dye removal from wastewater. RSC Adv 2020; 10: 8540-8547. https://doi.org/10.1039/D0RA01110J

[S6] Karthik G, Mohan S, Balakrishna RG. Engineering Ni-MOF/g-C_3N_4 composite-infused polysulfone membranes with optimal rejection, flux, antifouling, and photocatalytic properties for wastewater treatment. ACS EST Water 2024; 4: 4454-4463. https://doi.org/10.1021/acsestwater.4c00451

[S7] Maziya K, Kotze I, Richards HL. Enhancing dye rejection and antifouling resistance of thin film nanocomposite nanofiltration membranes by the incorporation of glutamic acid functionalized graphene oxide. Front Membr Sci Technol 2025; 4: 1571459. https://doi.org/10.3389/frmst.2025.1571459